Measurement of Collisional Rate Coefficients for Heliumlike Carbon Ions in a Plasma*

H.-J. KUNZE, A. H. GABRIEL,† AND HANS R. GRIEM
University of Maryland, College Park, Maryland
(Received 23 August 1967)

Measurements of the emitted line intensities from a θ pinch discharge are interpreted in terms of a modified corona model for heliumlike ions. The relative intensities of the resonance and intercombination lines have been measured for C V and O VII as a function of time, as has the absolute intensity of the *C* V 2^3S-2^3P multiplet. Electron temperatures and densities are obtained as functions of radius and time from the spectrum of Thomson-scattered laser light, and the densities also from Abel-inverted absolute continuum intensities. The derived model allows for population of the $n=2$ levels by direct impact excitation and by cascading, for collision-induced (exchange) transitions from $n=2$ triplets to singlets, and for collisional ionization from both the ground and the $n=2$ triplet levels. Collisional de-excitation of the triplets is shown to be negligible compared with exchange collisions and radiative transitions. Singlet excitation rates (near threshold) are derived with an accuracy of 40% which agree with Seaton and Van Regemorter's semiempirical formulas, triplet excitation rates which are smaller than the singlet rates by a factor 1.8 ± 0.2, and ground-state ionization rates to an accuracy of 25% agreeing with those estimated from the Born-exchange approximation for hydrogenic ions, suitably modified for two-electron systems. The measured value for the triplet-singlet exchange rate for C V is equal to $\frac{1}{3}$ of the value calculated for He I using the close-coupling approximation, and it has an estimated accuracy of 25%.

I. INTRODUCTION

WELL-DIAGNOSED transient plasmas with electron temperatures in the million degree range offer the opportunity of measuring rate coefficients (i.e., the product of cross section and initial electron velocity averaged over the electron-velocity distribution function) for excitation and ionization processes important in the quantitative analysis of, e.g., the spectra of the solar corona, or high-density, high-temperature laboratory plasmas. Such analyses are required both to determine the states of the hot plasmas and to assess radiative energy losses, mostly through resonance radiation in the vacuum ultraviolet or soft x-ray regions of the spectrum. Direct measurements of the corresponding electron-impact excitation and ionization cross sections for multiply ionized ions seem impractical, since the cross sections decrease rapidly with increasing charge ($\sim z^{-4}$), and because high-current ion beams are difficult to obtain. However, what is needed in most applications is the rate coefficients; but even when required for comparison with calculated cross sections, measurements of collisional rates in plasmas can yield rather direct information when the velocity distribution is measured from the spectrum of Thomson-scattered light in the relevant energy range for the process under study.

Several plasma sources have already been used for spectroscopic investigations of collisional rate coefficients, notably the Princeton Stellarator *C* for neon ions[1] (up to the lithium-like Ne VIII) and neutral helium,[2] the British Zeta for lithium-like ions[3] (mostly N V and O VI), and the Naval Research Laboratory Pharos Theta pinch for heliumlike O VII ions.[4] Heliumlike ions are particularly intriguing because of the relative simplicity of the spectrum and thus the increased chances of meaningful comparison with collision theory, compared with lower stages of ionization. This would be even more true for hydrogenic ions which, however, do not have strong lines as convenient to observe as the 2^3S_1–$2^3P_{0,1,2}$ lines of the heliumlike ions. These lines are exceedingly intense because the triplet levels are metastable and because the triplet excitation rate coefficients are comparable to those for the singlet system. Heliumlike ions are also especially interesting because they tend to be the only ionization stage of any significant abundance when their lines are first observed in a transient plasma. This is due to the relatively small ionization energies of lithiumlike ions, as compared with the excitation energies of heliumlike ions, which greatly reduces uncertainties in abundance determinations and therefore also in excitation rate coefficients obtained from absolute line intensities.

These excitation rate coefficients (for O VII) were first measured in the Pharos experiment.[4] The present paper reports on similar measurements with improved accuracy, due to the inclusion of Thomson scattering as a diagnostic technique, and on an extension to the measurement of ionization coefficients and the triplet-to-singlet exchange rate. While the present measurements are for C V and O VII, comparison with theory is made in such a way that the results should be of wider applicability. In the following, theoretical considerations are reviewed which lead to a modified-corona model for

* Jointly supported by the Atomic Energy Commission and the National Science Foundation.
† On leave from Culham Laboratory, England.
[1] E. Hinnov, J. Opt. Soc. Am. **56**, 1179 (1966).
[2] L. C. Johnson, Phys. Rev. **155**, 64 (1967).
[3] B. Boland, F. Jahoda, T. J. L. Jones, and R. W. P. McWhirter, *Proceedings of the Fourth International Conference on the Physics of Electronic and Atomic Collisions, Quebec, 1965*, edited by L. Kerwin and W. Fite (Science Bookcrafters, Hastings-on-Hudson, N. Y., 1965).
[4] R. C. Elton and W. W. Köppendörfer, Phys. Rev. **160**, 194 (1967).

heliumlike ions, and spectroscopic rate equations are derived which include all processes important in determining the observed spectrum. Theoretical estimates of relevant cross sections are then employed to obtain rate coefficients, either for subsequent comparison with experiment or to justify some approximations in the model.

The experimental sections include a description of the plasma source (a low-energy, large-diameter theta pinch), the diagnostic measurements (Thomson scattering and absolute and relative line and continuum measurements), and the measurements of resonance (1^1S_0–2^1P_1), intercombination (1^1S_0–2^3P_1), and 2^3S_1–$2^3P_{0,1,2}$ line intensities. These measurements are interpreted with the help of the modified-corona model. The results are summarized by comparing measured and calculated rate coefficients for singlet exitation and singlet ionization, and by deriving measured values for the triplet excitation coefficient and the coefficient for the $n=2$ triplet-to-singlet exchange process.

II. THEORY

A. Ionization

In transient plasmas with rapidly rising electron temperatures, the degree of ionization tends to lag behind the values corresponding to the so-called corona equilibrium. Lines of a given ionization stage are therefore observed at a temperature much higher (by about a factor of 2 in the present case) than in typical corona ionization equilibrium cases. This implies that recombination rates, which decrease with increasing temperature, are very much smaller than ionization rates, which increase exponentially with increasing temperature, even when dielectronic recombination[5] is considered in addition to the usual radiative recombination. The remaining, rate-controlling processes are indicated on Fig. 1.

Compared with the hydrogen corona excitation model, only the principal quantum number $n=2$ triplet levels will be significantly overpopulated, thereby introducing two additional processes for depopulating these levels, i.e., direct ionization and transfer to $n=2$ singlet levels, by collisions. Electron collision-induced transitions within the $n=2$ triplet group are for $N \gtrsim 2\times10^{16}(E'/E_H)^3(kT/E_H)^{1/2}$ cm^{-3} more likely than radiative transitions between $2^3P_{0,1,2}$ and 2^3S_1, E' and E_H being the energy differences of the 2^3S_1 and $2^3P_{0,1,2}$ levels and the hydrogen ionization energy, respectively, and T being the electron temperature. (This estimate is analogous to those performed in Refs. 6 and 7 to obtain validity criteria for local thermal equilibrium, but utilizes an effective Gaunt factor $\bar{g}\approx1$, as appropriate for the present value of E'/kT.) Moreover, since the relevant energy-level difference tends to be only of the order of 1% of thermal ion energies in these experiments, ion collisions are probably about as effective as electron collisions. Therefore, relative populations of the $n=2$ triplet levels should be governed by statistical weight factors for all densities fulfilling $N\gg10^{16}(E'/E_H)^3\times(kT/E_H)^{1/2}$ cm^{-3}. This criterion is satisfied by a factor $\gtrsim2$ for all experimental conditions reported in the present paper for which ionization via the triplet levels is at all important (more than ~20% of the direct ionization from the ground state). It therefore suffices to assume that the 2^3S_1, $2^3P_{0,1,2}$ levels have statistical populations, to use appropriate averages for the collisional and radiative depopulation coefficients, and to employ the sum of the excitation rate coefficients for all $n=2$ triplet levels, including a (small) correction for cascading. The near-statistical distribution in these levels cannot be significantly disturbed by collisional or radiative processes leading out of this group, because the corresponding rate processes within the group are all much faster. (Only for heavier heliumlike ions, radiative decay of 2^3P_1 to the ground state becomes more likely than to 2^3S_1.)

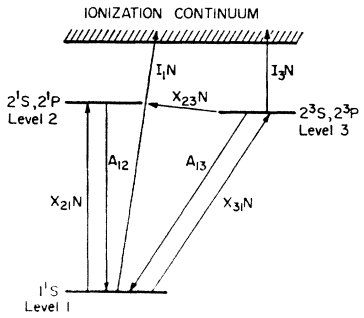

FIG. 1. Energy-level scheme for heliumlike ions, showing those processes taken into account in the present model.

[5] A. Burgess, Astrophys. J. **139**, 776 (1964).

The present model does not depend on a statistical population within the $n=2$ singlet levels, and these levels are treated together as one. Some relative overpopulation of the 2^1S level may occur, but is always much less than the triplet overpopulation.

We assume as an initial condition that practically all ions of the species under investigation are in the heliumlike ground state (density N_1). (This assumption is required only when considering ionization processes, and can be shown to be valid to better than 5%.) The appropriate rate equation accounting for both direct ionization and ionization from the metastable triplet levels (density N_3) by electron impacts (density N) is

$$dN_1/dt=-I_1NN_1-\alpha X_{31}NN_1. \quad (1)$$

Here I_1 and I_{31} are ground-state ionization and triplet excitation coefficients, and α is the relative probability that such excitation is followed by ionization. This

[6] R. Wilson, J. Quant. Spectr. Radiative Transfer **2**, 477 (1962).
[7] H. R. Griem, *Plasma Spectroscopy* (McGraw-Hill Book Company, Inc., New York, 1964), p. 150.

probability is approximately

$$\alpha \approx \frac{I_3 N}{A_{13}+(X_{23}+I_3)N}, \tag{2}$$

with the triplet ionization coefficient I_3, the transition probability A_{13} of the intercombination line, and the triplet-singlet exchange collision rate coefficient X_{23}.

B. Excitation

Characteristic times for changes in the ground-state density are, according to Eqs. (1) and (2),

$$\tau \equiv \frac{N_1}{dN_1/dt} \approx \left[\left(I_1+\frac{I_3 N}{A_{13}+(X_{23}+I_3)N}X_{31}\right)N\right]^{-1}, \tag{3}$$

which is of the order of microseconds in the present experiment. Characteristic times for changes in the excited-state densities (N_3), in contrast, are much shorter. They are at most of the order of radiative lifetimes (A_{13}^{-1}) of the metastable levels or, more generally, of the order $[A_{13}+(X_{23}+I_3)N]^{-1}$, which tends to be less than 0.1 μsec here. To express excited-state densities and accordingly also emission coefficients (ϵ) in terms of the ground-state densities, equilibrium excitation relations are therefore sufficient, e.g., for the resonance line (excitation energy E_{12} and excitation rate coefficient X_{21})

$$\epsilon_{12}=(E_{12}/4\pi)(X_{21}+\beta X_{31})N_1 N. \tag{4}$$

Here β is the relative probability that excitation of the triplet levels (coefficient X_{31}) is followed by excitation energy transfer to the excited singlet level (index 2), which then decays rapidly. In a manner analogous to Eq. (2), this probability is given by

$$\beta \approx \frac{X_{23}N}{A_{13}+(X_{23}+I_3)N}. \tag{5}$$

For the intercombination line, only triplet excitation need be considered, multiplied with the probability γ that this is followed by radiative decay to the ground state, i.e.,

$$\epsilon_{13}=(E_{13}/4\pi)\gamma X_{31} N_1 N, \tag{6}$$

with

$$\gamma \approx \frac{A_{13}}{A_{13}+(X_{23}+I_3)N}. \tag{7}$$

Easier to measure than the (absolute) emission coefficients of resonance and intercombination lines are their ratios,

$$\frac{\epsilon_{12}}{\epsilon_{13}} \approx \frac{X_{21}}{X_{31}}+\left[\frac{X_{23}}{A_{13}}\left(\frac{X_{21}}{X_{31}}+1\right)+\frac{I_3 X_{21}}{A_{13}X_{31}}\right]N \tag{8}$$

(using $E_{12}\approx E_{13}$), and the absolute value of the emission coefficient ϵ' for the 2^3S_1–$2^3P_{0,1,2}$ multiplet. This quantity is analogous to Eq. (6):

$$\epsilon' \approx \frac{E'}{4\pi}\frac{A'}{A_{13}+(X_{23}+I_3)N}X_{31}N_1 N, \tag{9}$$

where A' is the average over all $n=2$ triplet levels of the transition probability for the 2^3S_1–$2^3P_{0,1,2}$ transitions, i.e., $\frac{3}{4}$ of the usual transition probability.

According to Eq. (8), the ratio of resonance and intercombination line intensities measured at low densities is equal to the ratio of singlet and triplet excitation coefficients, and from the measured electron-density dependence of the line-intensity ratio the combination of terms contained in the square bracket can also be deduced. Using calculated radiative coefficients, this essentially yields the triplet-singlet exchange rate coefficient X_{23}, because according to the theoretical estimates for the triplet ionization rate coefficient I_3 (see the following section) its contribution is rather small. From measured emission coefficients ϵ' and Eq. (9) then follow absolute values for the excitation coefficients, inclusive of cascading. The measured decay times of the lines at ideally constant electron density and temperature (a method of correcting decay times for changes in density will be described in a later section) give with Eq. (3) the ionization coefficient I_1. Similar measurements at higher densities in principle yield an experimental value for I_3, the triplet-ionization coefficient, so that all collisional rate coefficients introduced in the present corona model may be derived rather directly from the observed quantities $\epsilon_{12}/\epsilon_{13}$, ϵ', and τ (the ionization time), and their electron-density dependence.

C. Errors and Corrections

As in the case of the ionization time, the simplifying assumptions made in the present model do not introduce any serious uncertainties into the relations for $\epsilon_{12}/\epsilon_{13}$ and ϵ'. When the density-dependent term in Eq. (8) is comparable to the first term, collisional and radiative rates within the $n=2$ triplet group are about equal. Relative populations in the $2^3P_{0,1,2}$ levels might then indeed be, e.g., 1:2 instead of 1:3, were they solely controlled by processes within this group. This would reduce the effective (averaged) value of A_{13} by a factor of 8/9 and increase that for X_{23} by a factor of $\frac{4}{3}$, were, e.g., triplet-singlet exchange collisions to involve ions in the 2^3S_1 state only. The quantity X_{23}/A_{13} would thus increase by as much as a factor of 1.5, while I_3/A_{13} should actually decrease by a small amount, ionization from S levels being more likely than from P levels by about a factor of 1.5. For this example, the quantity in square brackets could accordingly change by an estimated factor of 1.34, corresponding to a 17% increase in the line-intensity ratio. However, this constitutes an overestimate of errors introduced by assuming statistical populations for all four $n=2$ triplet levels. Actually the P levels will be preferentially populated from the

ground state, which offsets some of the drain through radiative transitions from P levels, whereas some of the overpopulation in the S level will be drained off through the collision-induced transitions to the singlet system. Theoretical errors in the line-intensity ratio due to the assumption of statistical populations are therefore probably no more than 10% in the case discussed and less than that at higher densities. Also at low densities, where the first term in Eq. (8) dominates, no significant errors are to be expected, because singlet and triplet cascading corrections would cancel, and for both lines excitation of S and P levels would be effective.

In Eq. (9), a cascading correction must of course be made to X_{31}, but other theoretical errors should again be small. This is suggested by the fact that at extremely low densities, where the density-dependent term in the denominator is small, the remaining factor is simply A'/A_{13}, whose (averaged) value is independent of the S-level population. Furthermore, as discussed above, averages of X_{23} and I_3 might be affected differently by an overpopulation in the S levels, and corresponding errors estimated analogously to those in Eq. (8) should be no more than $\sim 20\%$ for the conditions of the present experiment.

The cascading correction is essentially determined by the relative cross sections for the 1^1S_0 to 3^1P_1 and 1^1S_0 to 2^1P_1 excitations, which are in turn approximately proportional to the corresponding oscillator strengths. This consideration leads to an estimated 20% correction. Errors in such an estimate from neglecting higher levels and from increased excitation energies are in opposite directions and should therefore tend to cancel.

D. Collisional Rate Coefficients

For optically allowed dipole transitions the effective Gaunt factor modification of Van Regemorter[8] and Seaton[9] to the Bethe-Born approximation appears to constitute a good approximation to the electron-impact excitation cross sections even near threshold, if for ions the effective Gaunt factor is there chosen as $\bar{g}\approx 0.2$. The corresponding collisional rate coefficients assuming a Maxwellian electron velocity distribution are, e.g.,

$$X_{21}\approx 10\frac{ha_0}{m}\left(\frac{E_H}{kT}\right)^{1/2}\frac{E_H}{E_{12}}\bar{f}_{21}\exp\left(-\frac{E_{12}}{kT}\right), \quad (10)$$

where the error introduced by neglecting the actual, essentially logarithmic variation of $\bar{g}$[8,10] is less than 10% for $E_{12}/kT\gtrsim 1$. Also ,$\hbar$, a_0, and m have the usual meaning. To the calculated value[11] $f_{21}\approx 0.65$ for the resonance line oscillator strength the 20% cascading correction estimated above must be added and a similar amount to account for excitation of the 2^1S_0 level, judging from Coulomb-Born approximation results[12,13] for hydrogenic ions. The effective oscillator strength for the theoretical estimate of the singlet excitation coefficient is therefore $\bar{f}_{21}\approx 0.9$

To estimate the triplet ionization coefficient (ionization energy E_3), one may write in analogy to Eq. (10)

$$I_3\approx 10\frac{ha_0}{m}\left(\frac{E_H}{kT}\right)^{1/2}\exp\left(-\frac{E_3}{kT}\right)\int_0^\infty \frac{E_H}{(E_3+E)}\frac{df_3}{dE}\times\exp\left(-\frac{E}{kT}\right)dE, \quad (11)$$

ignoring exchange and introducing E as the final kinetic energy of the "ejected" electron. With the hydrogenlike value for the triplet continuum oscillator strength,

$$\frac{df_3}{dE}\approx\frac{2^3E_3^2}{3^{3/2}\pi(E_3+E)^3}, \quad (12)$$

and on integrating by parts a formula results like Eq. (10) with E_3 replacing E_{12} and an effective oscillator strength

$$\bar{f}_3\approx\frac{2^3}{3^{5/2}\pi}\left(1+\tfrac{1}{2}\frac{E_3}{kT}+\cdots\right), \quad (13)$$

i.e., $\bar{f}_3\approx 0.17$ for $kT\gg E_3$ or, e.g., $\bar{f}\approx 0.24$ for $kT\approx 2E_3$. However, the effective Gaunt factor[8,9] actually increases slowly for $kT\gtrsim 2E_3$, so that use of $\bar{f}_3\approx 0.30$ in Eq. (10) throughout the relevant temperature range should provide as good an approximation for the triplet ionization coefficient as for the singlet excitation coefficient. We therefore adopt

$$I_3\approx 3\frac{ha_0}{m}\left(\frac{E_H}{kT}\right)^{1/2}\frac{E_H}{E_3}\exp\left(-\frac{E_3}{kT}\right). \quad (14)$$

Most of the contribution to the integral in Eq. (11) comes from $E\lesssim E_3$; and for $kT\gtrsim 2E_3$, which is the usual situation, residual energies of the "colliding" electron thus tend to be larger than the kinetic energies of the "ejected" electron. Exchange effects should therefore not be too important.

For ground-state (near threshold) ionization the situation is different, and for heliumlike ions (other than for low z) it is probably best to estimate the coefficient I_1 from the Born-exchange approximation for hydrogenic ions,[14] multiplying by 2 to account for both bound electrons and using the actual ionization energy E_1 and

[8] H. Van Regemorter, Astrophys. J. **136**, 906 (1962).
[9] M. J. Seaton, in *Atomic and Molecular Processes*, edited by D. R. Bates (Academic Press Inc., New York, 1962), p. 414.
[10] C. W. Allen, *Astrophysical Quantities* (Athlone Press, London, 1963), 2nd ed., p. 42.
[11] W. L. Wiese, M. W. Smith, and B. M. Glennon, National Bureau of Standards. Report No. NSRDS-NBS-4, Vol. 1, 1966 (unpublished).
[12] J. Tully, M. Sc. Dissertation, University of London, 1960 (unpublished).
[13] A. Burgess, Mém. Soc. Roy. Sci. Liège 4, 299 (1961).
[14] M. R. H. Rudge and S. B. Schwartz, Proc. Phys. Soc. (London) **88**, 563 (1966); see also I. L. Beygman and L. A. Vainshtein, Soviet Astron. (to be published).

the charge z on the ion after ejecting the electron. In this manner, and making a numerical fit to the Maxwell average, it follows that

$$I_1 \approx 17 \frac{ha_0}{mz^2}\left(\frac{kT}{E_H}\right)^{1/2} \frac{E_H}{E_1+kT} \exp\left(-\frac{E_1}{kT}\right). \quad (15)$$

It is interesting to note that for $kT \approx E_1$ this expression agrees numerically with a relation obtained from Eq. (10) by using ionization instead of excitation energies and an effective oscillator strength 1.25, which is a very reasonable value and therefore lends further support to the estimate of the triplet ionization coefficient in Eq. (14).

For the triplet-singlet exchange collision rate coefficient no detailed calculations for heliumlike ions seem to exist. However, calculations[15] for neutral helium using the close-coupling approximation indicate an average cross section of $\sigma \approx 1.0\pi a_0^2 E_H/E$, if the electron energy E is in the range between $0.2E_H$ and $0.7E_H$. Assuming the usual z^2 scaling law for the equivalent energies to be valid, this corresponds rather well to the energy range relevant for the calculation of the triplet-singlet rate coefficient in typical plasmas. We therefore assume the same $1/E$ dependence to hold for all heliumlike ions. It remains to determine the z dependence of the cross section. In the absence of direct calculations, we note that our measured value for X_{23} (seen later) is smaller by a factor of ~ 5 than the rate coefficient corresponding to the above mentioned cross section for neutral helium. This suggests that for $z \lesssim 10$ the exchange cross section scales only as $1/z$ rather than as $1/z^2$ for the optically allowed transitions. With this scaling, the rate coefficient consistent with both the theoretical He I and measured C V values (see later) becomes

$$X_{23} \approx \frac{3.8}{z} \frac{ha_0}{m}\left(\frac{E_H}{kT}\right)^{1/2}. \quad (16)$$

This rate coefficient is much larger than, say, the singlet deexcitation coefficient to the ground state, which according to Eq. (10) and using detailed balancing would be smaller by a factor $\sim 3E_H/E_{12}$ for C V. Since the triplet excitation coefficient turns out be to about half the singlet excitation coefficient, and because of the larger statistical weight of the triplet levels, the triplet deexcitation coefficient to the ground state would be still smaller, say by $E_H/2E_{12}$, in comparison to the triplet-singlet exchange rate. Neglecting collisional deexcitation to the ground state therefore seems completely justified.

E. Radiative Rate Coefficients

Spontaneous transition probabilities for the 2^3S_1–$2^3P_{0,1,2}$ lines can be calculated to a rather high accuracy (~5%), as judged from the fact that "best" theoretical values of Weiss[11] agree to within ~10% with estimates employing hydrogenic-ion radial matrix elements. To obtain A', the calculated transition probability[11] for the multiplet 2^3S–2^3P must only be multiplied by $\frac{3}{4}$ to effect the appropriate average.

More problematical is the calculation of A_{13}, which is $\frac{1}{4}$ of the transition probability for the 1^1S_0–2^3P_1 intercombination line. It has been calculated recently[16] for He I to Ne IX, accounting for spin-orbit and spin-spin interactions and using Araki's[17] form for the energy matrix, including the off-diagonal terms. The values obtained are most likely within 20% of the true values, an accuracy which is suggested by comparison with a slightly less accurate calculation[18] using different off-diagonal energy matrix elements.

III. EXPERIMENT

A. Apparatus

The plasma used for these experiments was produced in a θ-pinch machine. This is described in detail elsewhere,[19] but the important parameters are as follows: The main bank of 9 kJ stored energy at 40 kV, was discharged through a single vacuum switch to a coil 30 cm long and 17 cm in diam. Bias field and preheater banks were discharged through the same coil. A peak compression field of 13 kG was obtained with a half-cycle duration of 3.6 μsec. A transparent fused silica discharge tube was used. A normal operation condition was established which was found to give a grossly stable and reproducible plasma. In this condition the tube was filled to an initial pressure of 12 mTorr of hydrogen, and a reverse bias field of 500 G was applied. This gave a plasma of 4.5 cm diam. with electron temperature and density of 220 eV and 4×10^{15} cm^{-3}, respectively. Photographic survey spectra revealed that the main impurities, in decreasing order of concentration, were oxygen, carbon, and silicon. Figure 2 shows typical time histories of the magnetic field, of C V and O VII lines, and of the continuum.

The coil was split in its midplane to allow several directions of viewing the plasma through the tube walls. Thus, light from a laser, scattered by the plasma, was viewed radially, as also were spectral line and continuum emission in the visible and quartz ultraviolet regions. At shorter wavelengths measurements were made axially using one of two instruments, a grazing incidence spectrometer or a plane crystal Bragg spectrometer. Absolute quantitative measurements were in all cases related to the plasma in the midplane of the coil, axial viewing being used only for relative measurements.

[15] P. G. Burke, A. J. Taylor, J. W. Cooper, and S. Ormande, in Fifth International Conference on the Physics of Electronic and Atomic Collisions, Leningrad, 1967 (unpublished).

[16] R. C. Elton, Astrophys. J. 148, 573 (1967).

[17] G. Araki, Proc. Phys. Math. Soc. Japan 19, 128 (1937).

[18] R. H. Garstang and L. J. Shamey, Astrophys. J. 148, 665 (1967).

[19] A. W. DeSilva and H.-J. Kunze (to be published).

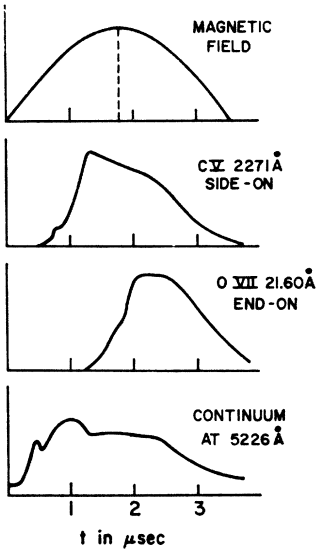

FIG. 2. Time variation of the magnetic field and some of the spectroscopic observations.

An independent monitor of the plasma conditions was provided by a quartz prism monochromator viewing the 2271 Å C v 2^3S_1–2^3P_2 line radially at the midplane. By observing the time of appearance, time of maximum intensity, decay rate, and peak intensity of this line, it was possible to reject those occasional discharges which did not meet the reproducibility requirements. In the case of other measurements of C v lines, it was also possible to use the intensity of this monitor to normalize the data and thereby to reduce the effective scatter. Since the diagnostic measurements could not in general be made simultaneously, this C v monitor has proved a most valuable facility.

In order to compare some of the data when taken at a higher electron density, a second operating condition was established. Here, the bank capacity was increased, raising the energy to 15 kJ and the peak field to 17 kG. Filling with 18 mTorr of hydrogen and using a bias field of 600 G, the density was increased to 6.5×10^{15} cm^{-3} and the electron temperature to 240 eV. Except where otherwise stated, all the measurements referred to were taken at the normal operating condition described previously for the 9 kJ bank.

B. Concentration of Impurity Elements

Measurements of excitation rates depend on a knowledge of the concentration of the element concerned, whether it occurs naturally as with carbon or oxygen, or whether it is deliberately added. At our low filling pressures, this is not a simple problem since selective injection or loss to the walls can be important during the preheater phase. (A detailed presentation of this effect will be given elsewhere.[20]) In carbon it was found that the addition of up to 5% of carbon atoms, in the form of methane, to the filling gas produced no change in the intensities of C III and C V lines during the main discharge. Above this concentration, however, a linear increase in intensities was observed. The slope in this linear region was therefore used to relate the intensity with no added carbon to a background carbon concentration. This level, produced by injection during the preheater, was found to be 1.3%. A similar experiment for oxygen did not show this loss effect. The intensity increase was linear from the start, and gave a background oxygen concentration of 3.6%.

C. Measurement of Electron Temperature and Density

Both of these parameters were measured as a function of radius and time in the midplane of the coil, using a scattering technique, a general description of which can be found, e.g., in Ref. 21.

The radiation from a Q-switched ruby laser, operated at power levels between 100 and 200 MW, passed axially along the discharge tube and was focused at the midplane of the coil. Light scattered by the plasma was observed at a scattering angle of 90°. The detecting system was a multichannel arrangement similar to that described in Ref. 22 and allowed the simultaneous measurement of seven portions of the spectrum. The laser head and the detecting system were mounted on a common carriage, permitting easy scanning of the scattering volume along a diameter of the plasma column.

The plasma conditions were such that no collective effects modified the spectrum, i.e., the spectrum reflected exactly the electron velocity distribution. In all cases a Gaussian shape of the spectrum was found, thereby justifying the assumption of a true kinetic electron temperature. In Fig. 3(a) the time history of the temperature on the axis is shown as well as the radial temperature distribution at two different timepoints. The experimental points are always average values of several discharges.

The determination of the electron density requires an absolute calibration of the scattered intensity. For this the Rayleigh scattering in N_2 was used.[23] By varying the laser power and the N_2 pressure in the discharge tube over a large range, the linearity of the Rayleigh scattered light showed that no breakdown processes or dust particles falsified the results. Figure 3(b) shows the electron-density distributions corresponding to the temperature values of Fig. 3(a).

Another value for the electron density can be obtained from the absolute intensity of the continuum emission in the visible. The diameter at the midplane of the discharge tube was imaged on a ½ meter grating mono-

[20] A. H. Gabriel and H.-J. Kunze (to be published).

[21] H.-J. Kunze, in *Plasma Diagnostics*, edited by Lochte-Holtgreven (North Holland Publishing Co., Amsterdam, to be published).

[22] H.-J. Kunze, Z. Naturforsch. **20a**, 801 (1965).

[23] R. D. Watson and M. K. Clark, Phys. Rev. Letters **14**, 1057 (1965).

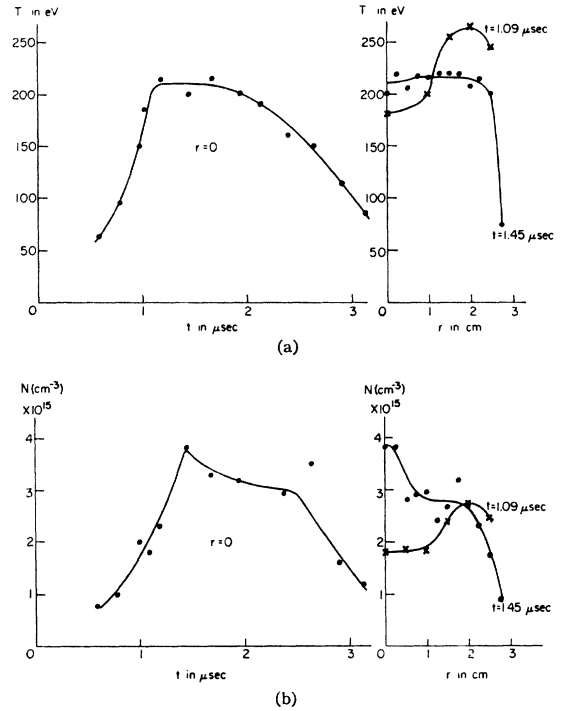

FIG. 3. Values obtained as a function of time t, and radius r, from the Thomson-scattering measurement; (a) for electron temperature T, and (b) for electron density N.

chromator. Radiation passing through the exit slit was divided by means of small mirrors into eight equal height elements and passed to separate multipliers. The monochromator had a bandwidth of 16 Å, and was set at 5226 Å, a region found to be free of line radiation. Previous measurements around 4976 Å, a region also quite often used for this purpose, yielded too high electron densities. Photoelectric scans revealed a series of weak lines appearing at the time of interest, which are not listed. It is assumed that these lines correspond to hydrogenlike transitions between levels of high principal quantum numbers of high ionization stages of the various impurity atoms. Such transitions are represented by groups of many closely spaced lines and may not be recognized on time-integrated photographic spectra when broadened by Stark and instrumental effects. The channel sensitivities were calibrated absolutely using the positive crater of a carbon arc, and its brightness as reported by Hattenburg[24] and Magdeburg.[25] The signals relating to surface brightness were first corrected for the discharge tube transmission, and then transformed to volume emission using the standard Abel integral equation. Density data were then calculated on the assumption of free-free emission, and corrected for the carbon and oxygen concentrations given above. The resulting density profile agreed with that obtained from light scattering, although the absolute values were somewhat higher. This can be attributed to neglecting corrections for silicon and other impurities. Silicon would be expected to ionize to a charge of X or XI so that a concentration of only 0.5% would give a 50% increase in the continuum intensity. In view of this factor, the density adopted was that obtained from the scattering data.

[24] A. T. Hattenburg, Appl. Opt. 6, 95 (1967).
[25] H. Magdeburg, Z. Naturforsch. **20a**, 980 (1965).

D. Spectral Intensities

The absolute intensity of the C V 2^3S_1–$2^3P_{0,1,2}$ multiplet was determined using the monochromator described above in connection with the continuum measurements. Due to the severe stray light problem associated with using the carbon arc at such short wavelengths, a second monochromator (a $\frac{1}{4}$-m grating instrument) was used as a predisperser for this measurement. A preliminary experiment demonstrated that the components of this multiplet had the expected statistical intensity ratio, and thereafter the bandwidth was set at 16 Å to accept all three components. After taking the Abel inversion, the radial profile was found to follow closely the continuum profile, thus verifying the assumption that the injected carbon is distributed uniformly through the plasma. The intensities were corrected for the measured transmission of the discharge tube wall which was found to be only 31% after several thousand discharges. In this way for the peak of C V (at 1.45 μsec from the initiation of the main discharge) an emission coefficient of $\epsilon' = 3.8$ W cm^{-3} sr^{-1} was obtained on the axis of the discharge tube, with an estimated error of ±20%.

Analysis according to the present corona model requires only a relative measurement of the intensities of the resonance 1^1S_0–2^1P_1 and intercombination 1^1S_0–2^3P_1 lines. Since these lines are very close in wavelength (40.27 and 40.73 Å in the case of C V), no intensity calibration of the spectrometer is required. Measurements were made photoelectrically using a Bragg and a grating spectrometer, and also photographically using the grating instrument. The Bragg instrument was a small device designed for solar observations and used an OHM crystal ($2d = 63$ Å) with a single entrance Soller collimator. For both instruments the detector consisted of a thin layer of p-terphenyl as scintillator in front of a 1P21 photomultiplier. In the case of the Bragg instrument, in addition, a filter combination was placed after the Soller collimator in order to preselect the wavelength range and thus to reduce the specular and diffuse reflected radiation from the crystal. Since no single filter exists having a transmission window around 40 Å, a combination of 2700 Å thick parlodion, 1400 Å aluminum, and 3600 Å indium was found to meet the requirements. This filter combination was supported on an 85% transmission fine nickel mesh. The grating instrument used a 2 m 1200 line per mm grating at an 86° angle of incidence in the first and second orders. For the photographic measurement emulsion calibration

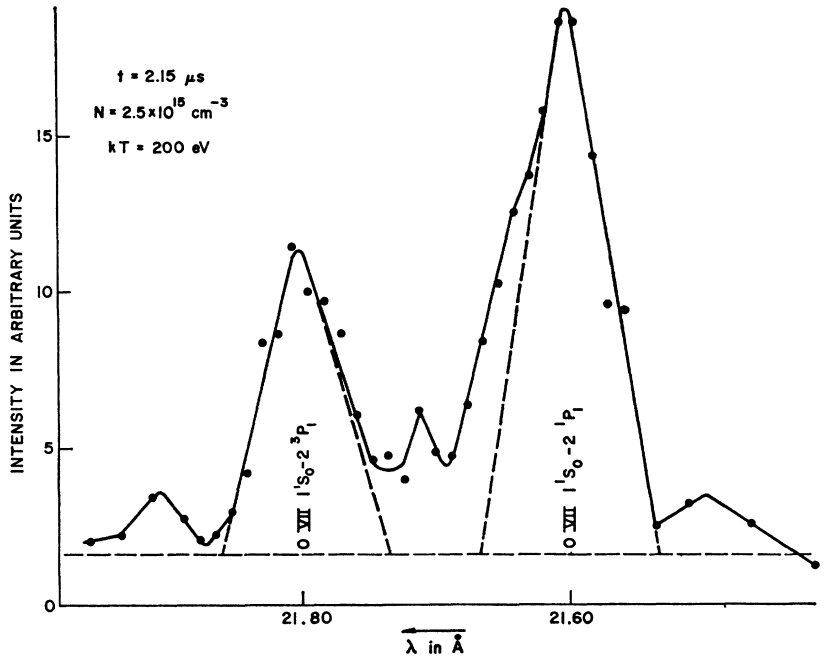

FIG. 4. A scan through the O VII resonance and intercombination lines recorded with the KAP crystal spectrometer.

was carried out using a fine mesh screen as a neutral filter. The time-integrated photographic measurement was justified, since the other measurements showed that for the normal discharge conditions there was no appreciable C V emission from later times in the discharge. All three measurements gave an intensity ratio resonance/intercombination line of 3.5±0.5. The grating photoelectric scan was repeated for the higher-density condition and then gave a ratio of 6.0±1.0 at the peak of C V. Finally the measurement was carried out for O VII using a KAP crystal ($2d=26.8$ Å) instead of the OHM crystal in the Bragg instrument, detector, and filter arrangement remaining the same. Figure 4 shows the intensity scan at 2.15 μsec after the beginning of the main discharge, each point representing an average value of several measurements. We obtain from this a value for $\epsilon_{12}/\epsilon_{13}$ of 1.8±0.2.

Measurements of the decay rate of C V were carried out on the 2^3S_1–$2^3P_{0,1,2}$ multiplet (see, e.g., Fig. 2). The signals at this wavelength were more intense and less troubled with photon noise fluctuations than the shorter wavelength lines. The C V monitor channel was used for this, leaving the ½-m monochromator free to measure the continuum radiation simultaneously. Only one of the continuum channels was used, and this viewed along a diameter, accepting light from approximately the same volume of plasma as the C V monitor. According to Eq. (9) the intensity of the C V multiplet is, to a first approximation, proportional to the square of the electron density; in addition, it depends on that plasma volume which is seen by the viewing optics. The continuum intensity (neglecting small changes in the contribution from impurity ions due to changing z) shows the same dependence. Therefore, if one takes the ratio of line to continuum intensity one is able to eliminate changes in the plasma geometry, plasma losses, and to a first approximation changes in density. In practice one simply subtracts from the measured decay rate of the line that of the continuum in order to obtain the true ionization rate $1/\tau$. After such correction the ionization time of C V was found to be 3.6 μsec (measured at 1.60 μsec) and 4.5 μsec (measured at 2.05 μsec) for the normal plasma and 1.7 μsec (measured at 2.35 μsec) for the high-density condition. The estimated experimental error is ±15% in the latter case, but 30% and 40% respectively for the first two values, since owing to a shorter lifetime of the plasma, the continuum corrections were considerable. The decay times of the lines were always measured sufficiently late after the peak, where residual ionization from C IV could not falsify the results. The short duration of the present plasma precluded meaningful measurements of the ionization time of O VII.

Finally, Table I shows a summary of the experimental results. The varying values of kT and N for these measurements are accounted for by the two operating conditions, the different times during the dis-

TABLE I. Measured quantities.

Ion	Quantity	Energy (kJ)	t(μsec)	kT(eV)	N(cm^{-3})
C V	$\epsilon'=3.8$ W cm^{-3} sr^{-1}±20%	9	1.45	210	3.8×10^{15}
	$\epsilon_{12}/\epsilon_{13}=3.5\pm0.5$	9	1.45	215	3.0×10^{15}
	$\tau=3.6$ μsec±30%	9	1.60	220	3.0×10^{15}
	$\tau=4.5$ μsec±40%	9	2.05	205	2.6×10^{15}
C V	$\epsilon_{12}/\epsilon_{13}=6.0\pm1.0$	15	1.80	240	6.5×10^{15}
	$\tau=1.7$ μsec±15%	15	2.35	240	6.5×10^{15}
O VII	$\epsilon_{12}/\epsilon_{13}=1.8\pm0.2$	9	2.15	200	2.5×10^{15}

charge, and whether on axis or spatially averaged parameters are relevant.

IV. INTERPRETATIONS

A. Line Intensities

The ion temperatures measured were always greater than electron temperatures,[19] and it can readily be shown that all the lines observed in the present experiment were optically thin. We can therefore proceed with the analysis without concern for problems of radiative transfer.

As can be seen from Eq. (8), measurement of $\epsilon_{12}/\epsilon_{13}$ at sufficiently low density gives a direct value for the ratio X_{21}/X_{31}. Such a low density could not be obtained for C v in the present experiment. However, one finds that for O vii, with a 20 times larger value of A_{13}, the present measurements are effectively at the low-density limit. There is a reasonable theoretical basis for the assumption that the ratio of the equivalent cross sections at threshold will not vary significantly along the isoelectronic sequence.[26] Since the O vii ratio measured here is consistent with an extrapolated value from our C v data we therefore adopt the value 1.8 for this ratio as valid throughout the sequence, and furthermore assume that (near threshold) it is independent of electron temperature. This value is further supported by line ratios of between 1.6 and 2.0 obtained for Ne ix in Scylla.[27]

Equation (8) predicts a linear variation of $\epsilon_{12}/\epsilon_{13}$ with N. The graph shown in Fig. 5 contains the two experimental points for C v together with the low-density limit discussed above. The slope of the best straight line through these gives the quantity in the square bracket in Eq. (8). Since the second term in this expression is small, a theoretical value for I_3 derived from Eq. (14) was used in order to derive a value for X_{23} of 1.13×10^{-9} cm^3 sec$^{-1}\pm25\%$.

It is interesting to reevaluate the O vii data from Pharos[4] in the light of the present model, using our experimental value of X_{23}, expressed in the form $8.6\times10^{-8}/z(kT)^{1/2}$. With $\epsilon_{12}/\epsilon_{13}$ measured as 2.5 ± 0.5 at $kT=250$ eV and $N=(6.2\pm1.5)\times10^{16}$ cm^{-3}, we obtain a value for X_{21}/X_{31} of 1.5 ± 0.5, which is consistent with the value derived here. The interpretation carried through in Ref. 4 is based on a similar model, but uses an estimated 2^3S to 2^1S transfer rate equivalent to a value of X_{23} which is only 60% of the value derived here.

[26] Near threshold, interactions are strong, so that a statistical model should apply, in which each of the three electrons is equally likely to leave the excited ion. We start with a singlet state, so that this model predicts a ratio of 2:1 for the singlet and triplet excitations, as a first approximation. Since this is close to the observed value, we consider it very unlikely that there could be a significant variation with z, say from B iv to Ne ix. As only values near threshold are involved in our rate coefficients, the temperature variation of this ratio, due to differences in energy dependence of the cross sections, will also be very small.

[27] G. A. Sawyer, F. C. Jahoda, F. L. Ribe, and T. F. Stratton, J. Quant. Spectr. Radiative Transfer 2, 467 (1962).

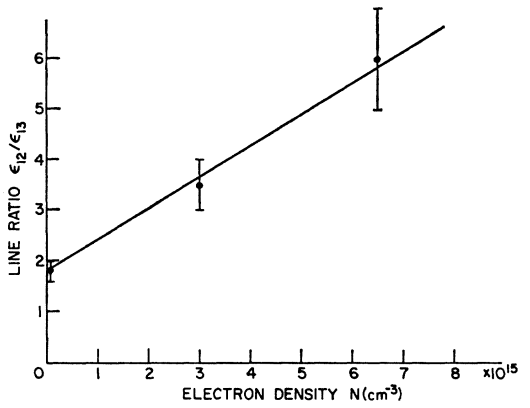

FIG. 5. The variation of $\epsilon_{12}/\epsilon_{13}$ with electron density N for C v.

It is now possible to derive a value for X_{21} from Eq. (9) using the measured value for ϵ', together with the above values for X_{23}, X_{21}/X_{31}, and a theoretical value from Eq. 14 for the correction term I_3. N_1 is calculated from the electron density and known carbon impurity concentration, and assuming that 83% of the carbon is in the C v ion at the time of peak C v emission. This figure of 83% was obtained by solving with a computer code the coupled rate equations for successive ionization of carbon in a homogeneous plasma with a mean T and N time history as measured for the experiment, and was found to be quite insensitive to variations in these parameters. The value obtained for X_{21} of 1.9×10^{-10} cm^3 sec$^{-1}\pm40\%$ agrees well with the theoretical value of 1.5×10^{-10} cm^3 sec^{-1} obtained from Eq. (10).

B. Ionization

Using Eq. (1) one can now derive values for I_1 from the measured decay times of the line intensities. For the correction term in Eq. (1) (which is $<20\%$ for all the present conditions) we use the above measured values for X_{23} and X_{21}/X_{31}, together with theoretical values for X_{12} and I_3 calculated as in Sec. II. In principle, with measurements at two values of N, it is possible to obtain an experimental value for I_3 also. However, since I_3 occurs only in the correction term, and we have a large error bracket on our low-density decay times, this was not possible in the present experiment. Three values of I_1 for C v were obtained corresponding to the values of τ given in the previous section.

V. SUMMARY AND CONCLUSIONS

Measurements have been made on the relative intensities of the resonance and intercombination lines of C v and O vii as a function of time and at two values of electron density, from a theta-pinch plasma. Absolute intensity measurements were made on the 2^3S–2^3P multiplet of C v, also as a function of time. These data have been analyzed using a modification of the usual

TABLE II. Rate coefficients for C V.

Coefficient	kT (eV)	Calculated (cm^3 sec^{-1})	Measured (cm^3 sec^{-1})	Measurement accuracy (%)
X_{23}	230	...	1.13×10^{-9} equivalent to $(8.6\times10^{-8})/z\sqrt{(kT)}$ with kT in eV	25
X_{21}[a]	210	1.5×10^{-10}	1.9×10^{-10}	40
I_1	220	6.4×10^{-11}	8.1×10^{-11}	35
	205	5.6×10^{-11}	7.6×10^{-11}	50
	240	7.5×10^{-11}	7.2×10^{-11}	25
I_3	210–240	4.7×10^{-10}	...	...
			$X_{21}/X_{31}=1.8$	10

[a] Both values for X_{21} include the contribution from cascade, estimated as 20%.

transient-corona model generalized for all heliumlike ions. Because of the small radiative transition probability from the 2^3P_1 level, two alternative depopulating processes for the $n=2$ triplet levels become important, i.e., ionization and, more important, collisional transfer to the $n=2$ singlet levels. Relative populations within the $n=2$ triplet levels are close to statistical and these levels are treated as one, as are also the $n=2$ singlet levels.

The measured rate coefficients derived from this analysis are given in Table II together with the values derived from theory. As can be seen, the resonance line excitation rate agrees with Seaton and Van Regemorter's semiempirical theory to within the experimental accuracy of 40%. Similarly, the ground-state ionization rate is in agreement with the value obtained from the hydrogenic Born-Exchange approximation (multiplied by 2 to account for the presence of two bound electrons) to within the experimental accuracy of 25%. The triplet-singlet exchange rate coefficient is equal to that given by the close-coupling result for neutral helium, divided by z, where $z-1$ is the charge on the ion. It should be noted that the value quoted for X_{23} in Table II relates to the entire $n=2$ triplet population. If it were assumed[4] e.g., that this all results from 2^3S_1 to 2^1S_0 transfer, then the rate coefficient for transfer from the 2^3S_1 level would be four times this value.

The ratio of singlet-to-triplet excitation rates is given by the ratio of resonance to intercombination line intensities in the low-density limit where the simple corona relations apply. The value measured in this way of 1.8 is expected to be valid for all heliumlike ions. In particular most astrophysical spectra (in particular of the sun) would satisfy conditions for the low-density limit for C V and higher sequence members, so that the line ratios observed would be expected to have this value, providing the source is optically thin. Measured values from the sun tend to support this prediction. Thus for O VII a line-intensity ratio has been measured[28] of 2.2 to $\sim$20% and for C V a value of 1.5 ± 0.5 was obtained. The latter figure was derived from an analysis of the OSO-III grazing-incidence spectra.[29]

Now that the important rate coefficients have been determined and generalized for the heliumlike sequence, it is possible to propose new diagnostic methods for the measurement of electron temperature and density, based upon the above model. Details of such methods are discussed fully in a separate paper.[30]

ACKNOWLEDGMENTS

The authors are grateful to Dr. W. M. Neupert for providing access to solar spectra from the OSO-III Satellite prior to publication. The OHM crystal used in our work was kindly made available by the Isomet Corporation. The computer time for this project was supported by National Aeronautics and Space Administration Grant No. NSG-398 to the Computer Science Center of the University of Maryland.

[28] R. L. Blake, T. A. Chubb, H. Friedman, and A. E. Unzicker, Astrophys. J. 142, 1 (1965).
[29] W. M. Neupert (unpublished).
[30] H.-J. Kunze, A. H. Gabriel, and H. R. Griem, Phys. Fluids (to be published).